

# Effect of Bio-Oil Species on Rheological Behaviors and Gasification Characteristics of Coal Bio-Oil Slurry Fuels

## Authors:

Ping Feng, Jie Li, Jinyu Wang, Huan Wang, Zhiqiang Xu

*Date Submitted:* 2021-02-22

*Keywords:* lignite, gasification, bio-oil, coal slurry, rheological behavior

## Abstract:

Bio-oil is a promising fuel as one of the main products from biomass fast pyrolysis for improving energy density and reducing transportation cost, but high acidity and low calorific value limit its direct application. It can be used to prepare coal bio-oil slurry as partial green fuels for potential feeds for synthesis gas production via gasification with the advantages over traditional coal-water slurries of calorific values and being additives-free. In the present work, three bio-oils were blended with lignite to prepare slurry fuels for the investigation of the effect of bio-oil species on rheological behaviors and gasification characteristics of coal bio-oil slurry fuels. Results show that slurry prepared with bio-oil from fruit tree pyrolysis is highly viscous and has higher activation energy in gasification. Slurries prepared with bio-oils from straw pyrolysis and pyroligneous acid from wood pyrolysis exhibited an acceptably lower viscosity, and the gasification temperatures were lower than for coal. The activation energy decreased by 15.98 KJ/mol and 2.77 KJ/mol, respectively, which indicates these bio-oils are more suitable with lignite for slurries preparation.

*Record Type:* Published Article

*Submitted To:* LAPSE (Living Archive for Process Systems Engineering)

*Citation (overall record, always the latest version):*

LAPSE:2021.0036

*Citation (this specific file, latest version):*

LAPSE:2021.0036-1

*Citation (this specific file, this version):*


LAPSE:2021.0036-1v1

*DOI of Published Version:* <https://doi.org/10.3390/pr8091045>

*License:* Creative Commons Attribution 4.0 International (CC BY 4.0)

Article

# Effect of Bio-Oil Species on Rheological Behaviors and Gasification Characteristics of Coal Bio-Oil Slurry Fuels

Ping Feng <sup>1,2,\*</sup> , Jie Li <sup>1</sup>, Jinyu Wang <sup>1</sup>, Huan Wang <sup>1</sup> and Zhiqiang Xu <sup>1</sup>

<sup>1</sup> Department of Chemical and Environmental Engineering, China University of Mining and Technology (Beijing), Beijing 100083, China; lijie0911@student.cumtb.edu.cn (J.L.); wjycumtb@163.com (J.W.); wanghuan@student.cumtb.edu.cn (H.W.); xzq@cumtb.edu.cn (Z.X.)

<sup>2</sup> State Key Laboratory of Multiphase Complex Systems, Institute of Process Engineering, Chinese Academy of Sciences, Beijing 100190, China

\* Correspondence: feng.ping@outlook.com

Received: 20 July 2020; Accepted: 24 August 2020; Published: 26 August 2020



**Abstract:** Bio-oil is a promising fuel as one of the main products from biomass fast pyrolysis for improving energy density and reducing transportation cost, but high acidity and low calorific value limit its direct application. It can be used to prepare coal bio-oil slurry as partial green fuels for potential feeds for synthesis gas production via gasification with the advantages over traditional coal-water slurries of calorific values and being additives-free. In the present work, three bio-oils were blended with lignite to prepare slurry fuels for the investigation of the effect of bio-oil species on rheological behaviors and gasification characteristics of coal bio-oil slurry fuels. Results show that slurry prepared with bio-oil from fruit tree pyrolysis is highly viscous and has higher activation energy in gasification. Slurries prepared with bio-oils from straw pyrolysis and pyroligneous acid from wood pyrolysis exhibited an acceptably lower viscosity, and the gasification temperatures were lower than for coal. The activation energy decreased by 15.98 KJ/mol and 2.77 KJ/mol, respectively, which indicates these bio-oils are more suitable with lignite for slurries preparation.

**Keywords:** bio-oil; coal slurry; rheological behavior; gasification; lignite

## 1. Introduction

Biomass is utilized to prevent the shortage of depletable fossil energy carriers [1] and is considered to be a renewable and carbon-neutral resource. Among various conversion technologies for biomass utilization, fast pyrolysis for producing pyrolysis liquids and char is an effective way to improve the energy density and reducing costs for vast gatherings [2]. Biomass pyrolysis liquids, also referred to as bio-oils, are complex mixtures of water, hundreds of organic compounds, and more or less solid particles [3]. Due to its complicated composition, lower heating value, and higher oxygen content and acidity, it cannot be used directly in combustion, extraction for fine chemicals, or transportation. Thus, it needs to be upgraded before utilization.

Using bio-oil for the preparation of slurry fuels has been promising in recent years. It could be used for preparation of slurry fuels with coal [4], biochar [5,6], or residual carbon floated from gasification slag [7]. The Process Engineering Chinese Academy of Sciences proposed using bio-oil and coal for slurry preparation as novel biofuels [4]. Bio-oils are employed as a liquid phase for the substitution of fluid in commercial coal water slurry aiming at both using the organic components providing calorific values and as additives for improving the viscosity and stability and further reducing the cost. Coal bio-oil slurries could be used for combustion for heat providing or gasification for syngas production [8–10].

The rheological behaviors and gasification characters have been reported based on containing a kind of bioslurry fuels. It was found that bio-oil from straw pyrolysis could be absorbed in char and form a highly viscous pumpable slurry [11]. Bio-oil and char from Mallee Biomass in Western Australia can form slurry fuels [12] and provides desirable fuel properties that meet specifications for combustion/gasification [13]. Even bio-oil-rich fractions were also suitable to be mixed with ground biochar for preparing bioslurry fuels [14]. The aging of bio-oil during storage significantly affects the viscosity and water content of slurries [6,15]. The gasification of char/coal bio-oil slurries has been reported [9,16–19]. It has been found that alkali metals and alkaline earth metals may contribute to higher syngas yields than co-gasification of individual bio-oil and char [19]. However, both rheology and gasification of slurry fuels were carried out based on a certain bio-oil and coal/char, while due to different types of parental biomass and different pyrolysis processes, the diversity of bio-oil is wide and the utilization of slurry fuels may vary significantly. Thus, understanding the effect of bio-oil species on peculiar features of rheology and gasification of slurry fuels is of great significance for fuel screening, optimizing operating conditions, and improving process efficiency [8].

To provide a broader way for the use of bio-oil and to support the development and operation of a commercial gasification process for bioslurry fuels, the effect of bio-oil species on rheological behaviors and gasification characteristics of coal bio-oil slurry fuels were investigated in the present research. Three typical bio-oils from pyrolysis of straw and husk, wood, and fruit trees were selected for preparation of coal bio-oil slurries. The gasification characteristics and estimated activation energy of bio-oils and coal bio-oil slurries were investigated under CO<sub>2</sub> atmosphere. The results may provide suggestions on the matching of bio-oil coals in regional areas and evaluation of the viability of a certain bio-oil for preparation of slurry fuels.

## 2. Materials and Methods

### 2.1. Coal and Bio-Oil Samples

Bio-oils used in experiments were purchased from Yineng Bioenergy Co., Ltd. (Anhui Province, China), which uses a fast pyrolysis reactor with solid heat carriers. In the pyrolysis system, biomass was sent to fast pyrolysis reactor together with a hot solid carrier (500 °C–800 °C) to produce pyrolysis gas and biochar in the absence of oxygen. The residence time of biomass was less than 3 s. Pyrolysis gas (around 400 °C–500 °C) were introduced to spray tower, and its temperature dropped below 40 °C at the exit. The mixture converged at the bottom of the spray tower and was pumped to the storage tank, and it appeared to be stratified after a period of settling. Bio-oils were collected in the storage tank. They are marked as bio-oil derived from straw and husk pyrolysis (BSR), bio-oil from pyrolytic acid (BPA), and bio-oil derived from fruit trees (BFT) respectively, in which BSR and BPA represent the middle layer (aqueous phase) and bottom layer (organic phase) of bio-oil produced from straw/husk pyrolysis, respectively, and BFT represents the bottom layer from fruit tree pyrolysis. The components of bio-oils were measured by GC-MS (3800GC/300MS, Varian, Palo Alto, CA, U.S.A.), and the results are listed in Table S1 in Supplementary Materials. The densities of samples were determined by measuring the mass of fuels at a constant volume using a 1 mL volumetric flask, and they were 1.011 g/cm<sup>3</sup>, 1.0935 g/cm<sup>3</sup>, and 1.1209 g/cm<sup>3</sup> for BPA, BSR, and BFT, respectively. The standard deviation of density is less than 5%. The water content of bio-oils was measured by Karl Fischer Titrator (V30, Mettler Toledo, OH, USA), and they were 9.50%, 45.54%, and 74.15%, respectively, for BPA, BSR and BFT. The ash contents of BPA, PSR, and BFT were measured following ASTM D482-95, and they were 0.10%, 0.12%, and 2.91%, respectively.

Lignite from Xilin Gol league mining area was used for biofuels preparation. Coal sample was crushed and then ball-milled for more than 2 h until particles passed through 200 meshes. The particle size distribution is shown in Figure 1. The proximate analysis and ultimate analysis of lignite are shown in Table 1.

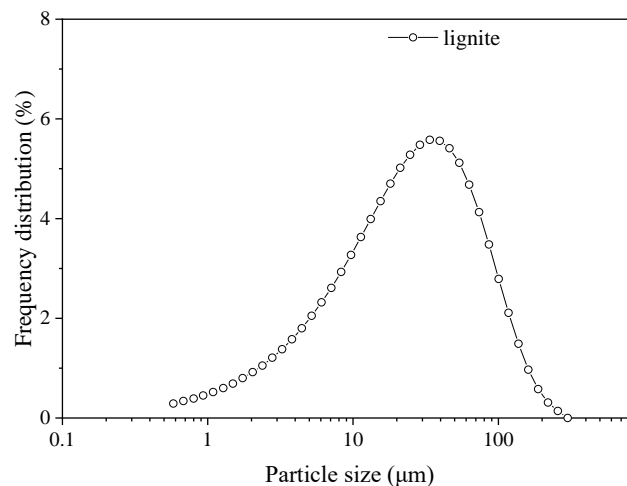


**Figure 1.** Particle size distribution of lignite.

**Table 1.** Proximate and ultimate analysis of lignite.

Samples	Proximate Analysis				Ultimate Analysis				
	$M_{ad}$ *	$A_d$	$V_{daf}$	$FC_d$	$C_{daf}$	$H_{daf}$	$O_{daf}$	$N_{daf}$	$S_{t,d}$
	%	%	%	%	%	%	%	%	%
Lignite	1.77	20.83	45.3	43.31	70.32	4.20	25.74	0.99	0.42

\* ad represents air-dried basis, d represents dry basis, and daf represents dry ash-free basis.

## 2.2. Bioslurry Preparation

Before slurry preparation, lignite was dried in an oven at 105 °C for 24 h. Slurry preparation was conducted by adding lignite powders into slowly stirred bio-oils in order to minimize the carrying of gas into the slurries. The concentration is defined by the mass ratio of coal to slurry in the research. The mixtures were then stirred at a high speed of 1000 r/min for 10 min for the acquisition of homogeneous slurries. The experiments were all based on fresh slurries since their properties may change after long-time storage.

## 2.3. CO<sub>2</sub> Gasification Experiments

The CO<sub>2</sub> gasification of bio-oils, lignite, and biofuels was carried out in a thermal gravimetric balance (STA409PG, NETZSCH, Gerätebau, Germany). Ten milligrams of samples were put in an alumina crucible and then placed in the furnace with 30 °C for 10 min at CO<sub>2</sub> atmosphere and then programmed-temperature-heated from 30 °C to 1200 °C at a heating rate of 20 °C/min as illustrated in Figure 2. Bio-oils and slurries were put in the crucible by extruding the droplets through a micro sampler. Before the start of experiments, CO<sub>2</sub> was introduced into the furnace for ten minutes to displace the air therein. The CO<sub>2</sub> flow rate in experiments was set to 50 mL/min. When the temperature reached 1200 °C, the atmosphere in the furnace was switched to nitrogen and the sample was cooled down. Each experiment was replicated three times to minimize standard deviations.

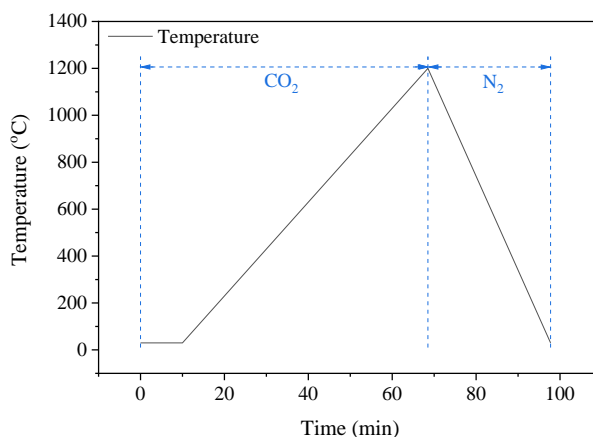


**Figure 2.** Temperature program of TG (thermal gravimetric) analysis.

### 3. Results and Discussion

#### 3.1. Rheological Behaviors

Pumping and transporting are crucial processes prior to gasification or combustion. The rheological behaviors of slurry fuels with different coal concentrations were measured. Due to the very high apparent viscosity of coal BFT slurry that cannot be measured at room temperature, Figure 3 only presents the evolution of rheological characteristics of the other bioslurries with different concentrations, and Figure 4a presents the rheological behavior of coal BFT slurry at an elevated temperature of 70 °C. All of the slurry fuels exhibit apparent shear-thinning characteristics below 50 s<sup>-1</sup>, which is consistent with other slurries. This is attributed to the breakdown of the gel structure of the mixture [6]. The apparent viscosity tends to be stable as the shear rate reaches 100 s<sup>-1</sup>. It is also remarkable that the increase in solid concentration of slurry contributes to the increase of apparent viscosity. With similar viscosity (around 850 mPa·s) and at a shear rate of 100 s<sup>-1</sup>, the coal loading of coal BSR slurry is 34%, while it is 48% for coal BPA slurry. This indicates that in industrial applications, coal BPA may carry more coal to form slurry fuels and the heating values are more likely to be higher. Figure 4a shows the rheological behavior of coal BFT slurry with 10% coal concentration. Although the concentration of coal BFT slurry is significantly lower than the other two slurries, its apparent viscosity reaches 2589 mPa·s, far exceeding the viscosity of the other two slurries with 36% coal concentration at room temperature. This shows that during BFT slurry preparation, the amount of coal added is extremely limited, and the viscosity is high even at 70 °C, which is not suitable for preparing slurry fuels.

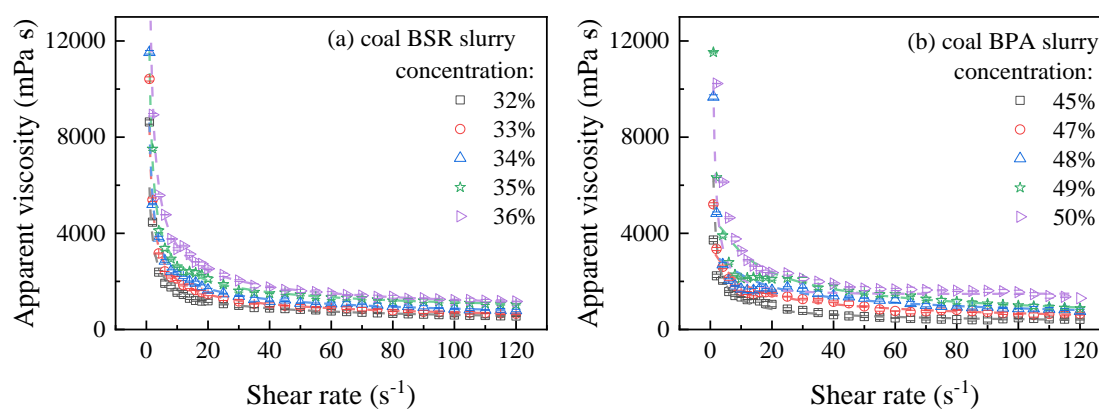


**Figure 3.** Apparent viscosity of slurry fuels as a function of the shear rate. (a) Coal bio-oil derived from straw and husk pyrolysis (BSR) slurries with coal concentrations from 32% to 36%, (b) coal bio-oil from pyrolygneous acid (BPA) slurries with coal concentrations from 45% to 50%.

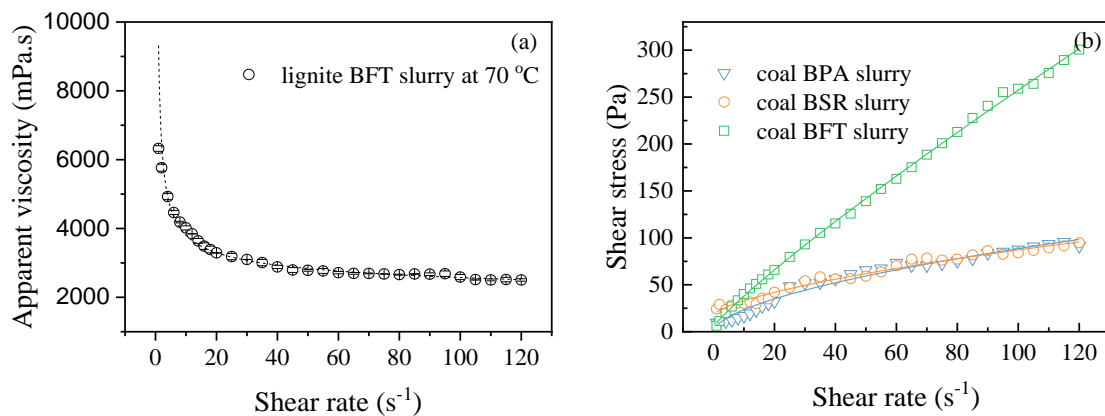


**Figure 4.** (a) Apparent viscosity of coal bio-oil derived from fruit trees pyrolysis (BFT) slurry (with concentration of 10%) as a function of the shear rate at 70 °C. (b) Shear stress of slurry fuels as a function of the shear rate.

The Herschel–Bulkley model was used to fit the rheological model of coal bio-oil slurry shown in Figure 4b, and the fitting parameters are shown in Table 2.

$$\tau = \tau_0 + k\gamma^n \quad (1)$$

where  $\tau$  is shear stress,  $\tau_0$  is yield stress,  $k$  is consistency factor,  $\gamma$  is shear rate, and  $n$  is flow index.

**Table 2.** Rheological index of different bio-oil coal slurry.

Sample	$\tau_0$	$k$	$n$	$R^2$
Coal BPA slurry	4.84	6.21	0.58	0.97605
Coal BSR slurry	16.93	3.66	0.64	0.97775
Coal BFT slurry	5.00	4.32	0.88	0.9991

The rheological curve fitting coefficient  $R^2$  of slurries is close to 1, which confirms that the Herschel–Bulkley model may describe the coal bio-oil slurries. The flow characteristic index  $n$  is less than 1, which implies that the slurry fuels exhibit a yield of pseudoplastic fluid. The  $K$  value of coal BPA slurry is larger than that of coal BSR slurry and coal BFT slurry, and the  $n$  value is smaller than that of other slurries, indicating that coal BPA slurry is the most pseudoplastic. In industrial applications, slurry fuels are expected to have a higher solid content and heating value, but at the same time, this also brings about an increase in viscosity. Therefore, efforts were then taken to carry out further work for reduction in viscosity.

Coal bio-oil slurries are thermodynamically unstable systems, which are significantly affected by temperature. The aforementioned coal BFT slurry with an excessively high viscosity that could not be measured at room temperature decreased to 2589 mPa·s when the temperature was increased to 70 °C. The temperature–viscosity relation was shown in Figure 5a. The apparent viscosity of all slurries decreases as the temperature increases. Coal BPA slurry is more sensitive to temperature, and its apparent viscosity decreased from 725 mPa·s at 25 °C to 249 mPa·s at 60 °C. It has been reported that the increase in temperature will cause the viscosity of the liquid phase bio-oil to decrease significantly. The viscosity change of the coal bio-oil slurry has a good correlation with the change of the viscosity of bio-oil, which is the main factor that causes the reduction in viscosity [4]. Furthermore, the difference in the thermal expansion characteristics of the liquid and solid phases leads to an increase in the volume share of free water; that is, the expansion rate of the liquid phase is higher than that of the solid phase under the heating state, resulting in a decrease in the viscosity of coal slurry. Scholars [19–21] found that the influence of temperature on the apparent viscosity of coal–water slurries can be fitted with the

Arrhenius equation as shown in Equation (2). The equation was also applied for coal bio-oil slurries, and the results were shown in Figure 5b. It can be seen that the Arrhenius equation fits well with all slurries, which indicates that the influence of temperature on the apparent viscosity of the coal bio-oil slurries could also be described by the Arrhenius equation.

$$\ln \mu = \ln C_1 + C_2/T \quad (2)$$

where  $\mu$  represents apparent viscosity,  $C_1$  and  $C_2$  are constant, and  $T$  represents temperature, K.

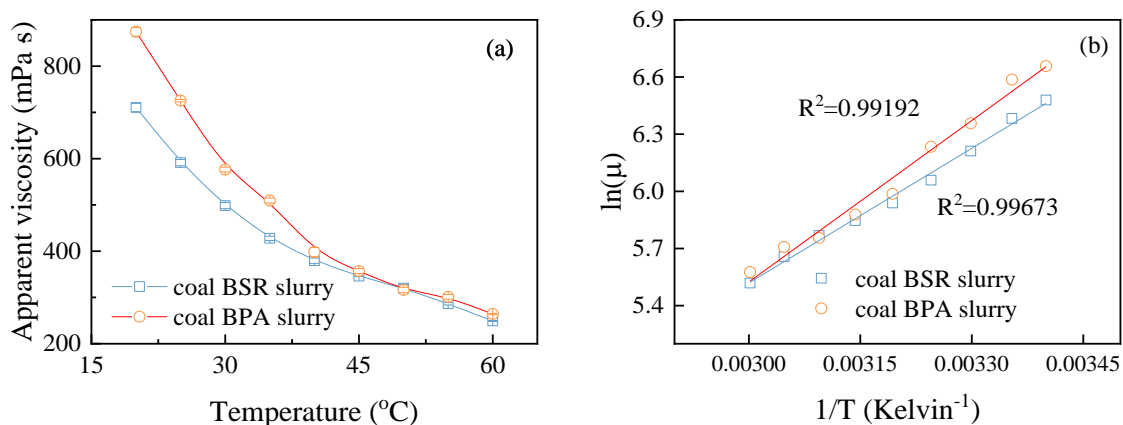


**Figure 5.** (a) Comparison of temperature–viscosity characteristics of coal BPA slurry (with concentration of 48%) and coal BSR slurry (with concentration of 33%). (b) Arrhenius fitting of temperature–viscosity relationship.

### 3.2. Gasification of Slurry Fuels

The process of gasification in a thermobalance is widely used in gasification and reaction kinetics studies [22–24]. The TG and DTG (Derivative Thermogravimetric) curves of CO<sub>2</sub> gasification of bio-oils are presented in Figure 6. After gasification, residual char was also seen in Figure 6a, which shows higher yield for BFT and lower yields for BSR and BPA as observed. This is related to the ash content of the bio-oils. BFT is the most viscous and has more ash and heavy organic matters than the others; thus its residual char yield is higher. The weight loss process of individual bio-oil took place in three stages, namely the volatile removing stage, CO<sub>2</sub>-pyrolysis, and gasification stages. The temperature range and weight loss of these three stages may vary for the compositions of fuels. Moreover, the reactions that occurred in each stage may cross each other, which blurs the boundaries of stages. For BSR and BPA, the light volatile removing stage (referred to as stage 1) occurred at a temperature around 100 °C, which is mainly devolatilization (evaporation of H<sub>2</sub>O and small organic matter), decomposition, and char formation gradually at the end of this stage. It was then followed by the pyrolysis stage (referred to as stage 2) which occurs below 600 °C [2,25–27]. For BFT, as seen in Figure 6b, the first two stages were joined as it shows three continuous weight losses between 100 °C to 600 °C. The pyrolysis of heavier components in BFT is likely to occur in this range. The last stage (referred to as stage 3) took place above 600 °C, and the carbon in bio-oils and newly formed char reacted with CO<sub>2</sub> introduced in the furnace. The TG curves of individual bio-oils indicate that BFT had higher mass loss compared to the other bio-oils owing to its higher carbon content and higher content of heavy organic matter. Since the carbon content of BPA is relatively low, the carbon gasification in the third stage was neglectable.

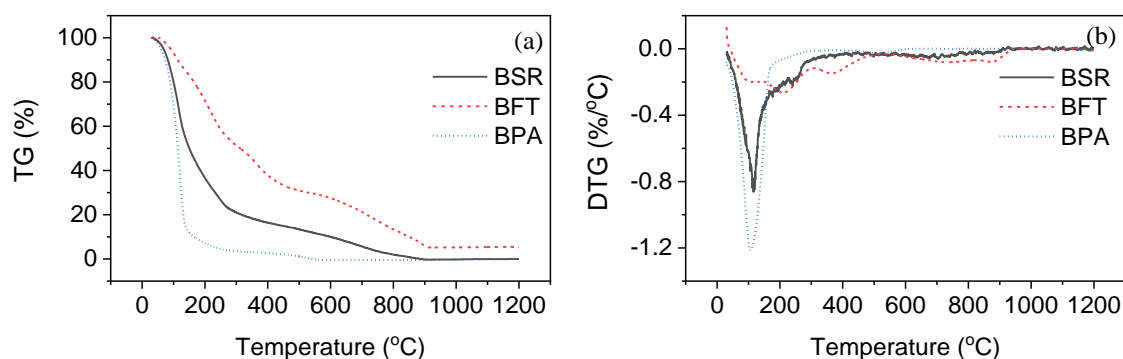


**Figure 6.** (a) TG curves of gasification of bio-oils; (b) DTG curves of gasification of bio-oils.

Lignite was added into bio-oils for preparation of bioslurries, and the TG and DTG curves of lignite are shown in Figure 7. The three stages of CO<sub>2</sub> gasification of lignite are also seen in Figure 7b. The first stage also concentrates at 100 °C, representing the moisture removal of lignite. The second stage ranges from 200 °C to 700 °C, where the pyrolysis of lignite occurs. The last stage (700–1020 °C) is the CO<sub>2</sub> gasification, where the char was gasified.

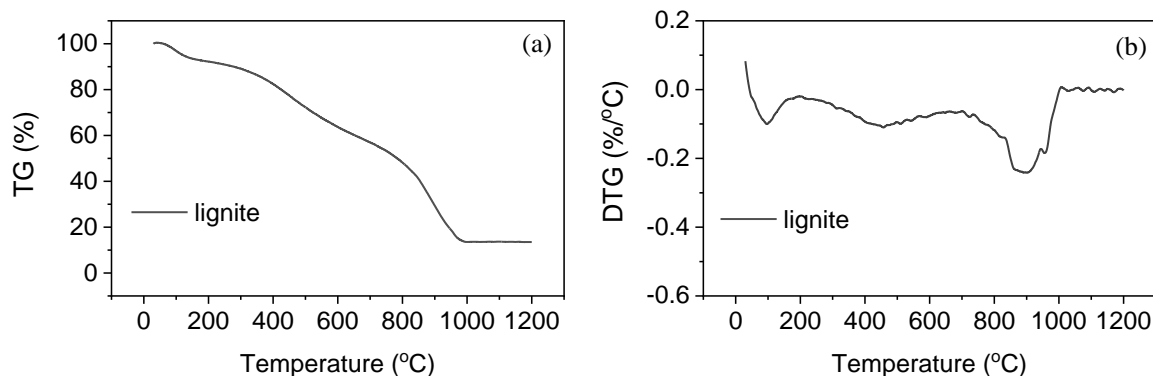


**Figure 7.** (a) TG curves of gasification of lignite; (b) DTG curves of gasification of lignite.

The gasification reactivity of fuels was quantitatively evaluated by gasification performance indices, which can be obtained from the TG and DTG curves, such as the final weight loss temperature ( $T_f$ ) and temperature at which the maximum weight loss rate in each stage ( $T_{m1}$ ,  $T_{m2}$ ,  $T_{m3}$  for stages 1 to 3, respectively) [28]. Among the  $T_{m_s}$ ,  $T_{m3}$  represents the peak temperature at the maximum weight loss rate in CO<sub>2</sub> gasification and needs special attention in comparison.

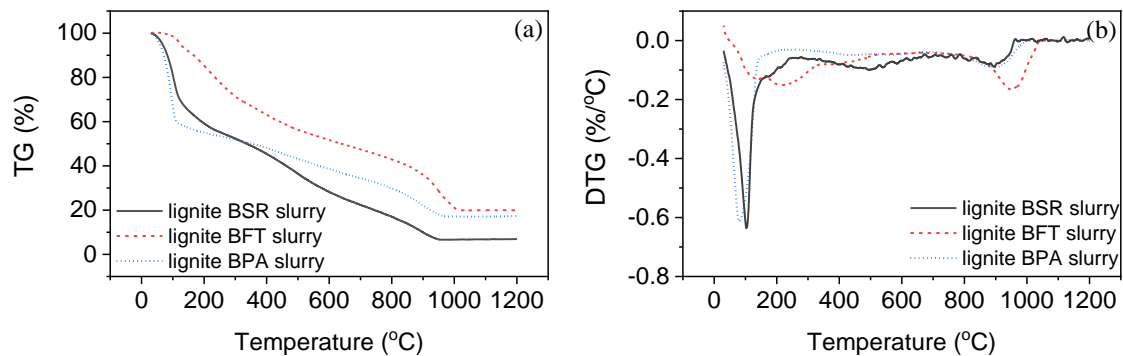
Gasification performance indices of individual fuels were shown in Table 3. There is no obvious gasification stage for BPA, and its  $T_{m3}$  and  $T_f$  are not listed.  $T_{m1}$  for the bio-oils is higher than for lignite. In the first stage of gasification, moisture and gases are removed from lignite, while in bio-oils, both water and other organic molecules volatilized and cause a wider and delayed peak temperature in this stage. The advances in gasification of bio-oils over lignite were concentrated in the gasification stage, as they give lower  $T_{m3}$  and  $T_f$ . This indicates that carbon in bio-oil is more reactive than lignite, and by mixing bio-oils and lignite, the gasification may improve, which is investigated in the next section.

The biofuels were prepared by mixing lignite with individual bio-oil, and their TG and DTG curves are shown in Figure 8. They show comprehensive characteristics with lignite and bio-oils. Similarly, the gasification of biofuels could also be divided into three stages. Compared with BFT, the peak temperatures of lignite BFT slurry in three stages were delayed by 20 °C or even longer. This indicates that the coal particles in BFT to some extent inhibit the gasification of liquids.  $T_f$  was also delayed for 20 to 60 °C. This phenomenon could also be proved by comparing the  $T_{m3}$  of BSR, BPA, and the slurries prepared by them.



**Table 3.** Gasification performance indices of individual fuels.

Sample	T <sub>m1</sub> (°C)	T <sub>m2</sub> (°C)	T <sub>m3</sub> (°C)	T <sub>f</sub> (°C)
BSR	116	238	705	914
BPA	107	521	-	-
BFT	121	209/363	733/876	939
lignite	97	457	899	1021

**Figure 8.** (a) TG curves of gasification of coals; (b) DTG curves of gasification of bio-oils.

The characterization of temperature during gasification of biofuels is shown in Table 4. The biofuels have T<sub>m3</sub>s ranging from 895 °C to 959 °C, which implies that the addition of bio-oil has different effects on lignite gasification. Compared with lignite, T<sub>m3</sub> of lignite BFT slurry was delayed for 60 °C, and T<sub>m3</sub> of lignite BSR slurry and lignite BPA slurry remain almost the same. However, T<sub>f</sub>s of all bio slurries move in advance. This implies that the gasification was compressed in a shorter range of temperature and that the gasification does not require temperatures as high as for lignite.

**Table 4.** Gasification performance indices of biofuels.

Sample	T <sub>m1</sub> (°C)	T <sub>m2</sub> (°C)	T <sub>m3</sub> (°C)	T <sub>f</sub> (°C)
lignite BSR slurry	103	498	895	967
lignite BPA slurry	81	428	898	1000
lignite BFT slurry	137	215/367	959	1041

### 3.3. Thermodynamic Analysis

The kinetics of gasification is known to be complicated since gasification of coal, bio-oil, and biofuels is a heterogeneous action. In the present research, activation energy ( $E$ ) is estimated by a non-isothermal single heating rate method. DTG data under this circumstance could be used to calculate kinetic parameters by the Coats–Redfern method. The kinetics of reaction is described by Equation (3):

$$\frac{d\alpha}{dt} = A \exp\left(-\frac{E}{RT}\right) \cdot f(\alpha) \quad (3)$$

in which  $T$  is the sample temperature, K;  $\alpha$  is the extent of conversion, %;  $f(\alpha)$  is the hypothetical model of the reaction mechanism;  $A$  is the frequency factor;  $E$  is the apparent activation energy,  $\text{kJ}\cdot\text{mol}^{-1}$ ;  $R$  is the gas constant and equals  $8.314 \text{ J}\cdot\text{mol}^{-1}\cdot\text{K}^{-1}$ ; and  $t$  is time, s.

Based on TG curves,  $\alpha$  can be described by Equation (4):

$$\alpha = \frac{W_0 - W}{W_0 - W_f} \quad (4)$$

in which  $W_0$  is the initial weight of sample,  $W$  is the weight at time  $t$ , and  $W_f$  is the residual mass after gasification.

As the heating rate  $\beta$  ( $\beta = dT/dt$ ) is constant during gasification, Equation (1) can be expressed as Equation (5):

$$\frac{d\alpha}{dT} = \frac{A}{\beta} \exp\left(-\frac{E}{RT}\right) \cdot f(\alpha) \quad (5)$$

Normally, it is assumed that the main gasification process can be described by first-order kinetics. Thus,  $f(\alpha)$  is substituted by  $(1 - \alpha)$ . The equation derived for calculating activation energy is given as Equation (6):

$$\log\left[-\frac{\ln(1-\alpha)}{T^2}\right] = \log \frac{AR}{\beta E} - \frac{E}{2.3RT} \quad (6)$$

where  $E$  and  $A$  can be calculated from the slope and intercept of a plot of  $\log\left[-\frac{\ln(1-\alpha)}{T^2}\right]$  against  $\frac{1}{T}$ .

The fitting curves of Arrhenius diagram of fuels for calculating  $E$  and  $A$  were shown in Figure 9, and the estimated results were shown in Table 5. The fitting curves of lignite BSR slurry, lignite BFT slurry, and lignite BPA slurry lay on both sides of the lignite gasification curve, which indicates that the three bio-oils have different effects on gasification of biofuels. A noticeable decrease in  $E$  occurred in lignite BSR slurry and lignite BPA slurry compared to lignite; in particular, for lignite BSR slurry, the activation energy is reduced by 15.98 kJ/mol. This means the co-gasification of lignite and BSR or BPA needs less energy than lignite with lower  $E$ , which is inconsistent with lower  $T_f$  of these slurries than lignite showing synergetic effects. During the heating process, due to the addition of liquid, micro-explosions may occur in the slurry fuel droplets, resulting in an increase in the reaction area and reaction rate. There is also literature that shows that alkali metals and alkaline earth metals have a catalytic role in the gasification process, which can increase the reaction rate of carbon.

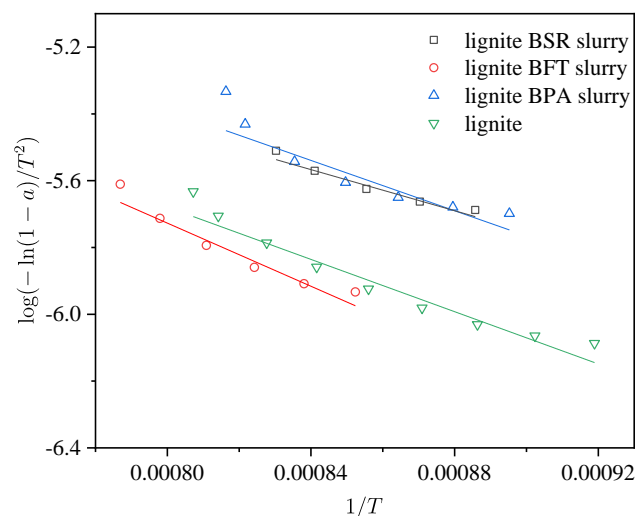


Figure 9. Arrhenius diagram of slurry fuels and coal sample.

Table 5. Activated energy of samples.

Sample	Temperature Range (°C)	$E$ (kJ·mol <sup>-1</sup> )	$A$ ( $\times 10^{-4}$ s <sup>-1</sup> )	$R^2$
lignite BSR slurry	856–931	58.84	2.46	0.96
lignite BFT slurry	900–998	90.40	41.13	0.96
lignite BPA slurry	844–953	72.05	12.19	0.95
lignite	815–966	74.82	8.47	0.96

Lignite BFT slurry lies on the opposite side and has higher  $E$  than lignite and other slurries. This is also proven by lignite BFT slurry having delayed  $T_{m3}$  compared to lignite. This seems to contradict the conclusions of the two previous slurries, because lignite BFT slurry may also contain

alkali metals and microburst during high-temperature processes. However, in this case, the differences between the three bio-oils must be considered. Compared with BPA and BSR, BFT has lower water content, higher viscosity, higher density, and more heavy components. During the early heating process, the heavy components are less volatilized and surround the coal particle surface more. The droplets formed are larger and denser, which hinders the heat and mass transfer of coal particles in high-temperature regions, which in turn causes the higher gasification reaction temperature.

#### 4. Conclusions

Three bio-oils (BSR, BPA, and BFT) were used for preparation of coal bio-oil slurries, and the effect of bio-oil species on rheological behavior and CO<sub>2</sub> gasification characteristics of coal bio-oil slurries were investigated. Among the coal slurries of the same concentration, the slurry prepared by BPA has the lowest apparent viscosity, and its coal concentration reaches at least 45%. The slurry prepared by BFT has the highest viscosity, and it cannot flow at room temperature. Increasing the temperature is beneficial to reducing the viscosity, and the relation of apparent viscosity and temperature for slurries conforms to the Arrhenius equation. All bio-oil shows lower gasification temperature than lignite. By preparing biofuels, BPA and BFT present a synergetic effect with lignite by reducing the  $T_{m3}$  and  $T_f$ . However, the gasification of lignite BFT slurries lags at high-temperature areas compared with lignite. In thermodynamic calculations, the activation energy of lignite BSR slurry and lignite BPA slurry is reduced by 15.98 KJ/mol and 2.77 KJ/mol, respectively. In summary, the BSR and BPA are recommended for bioslurry preparation considering both the rheological properties and gasification properties.

**Supplementary Materials:** The following are available online at <http://www.mdpi.com/2227-9717/8/9/1045/s1>, Table S1. Components of bio-oils in the experiments.

**Author Contributions:** Writing—original draft preparation, P.F.; project administration, P.F.; supervision, P.F.; experimental investigation, J.L., J.W., H.W.; supervision, Z.X. All authors have read and agreed to the published version of the manuscript.

**Funding:** This research was funded by Open Research Fund of State Key Laboratory of Multiphase Complex Systems (grant number MPCs-2017-D-12) and National Natural Science Foundation of China (grant number 51604281) and the Fundamental Research Funds for the Central Universities (grant number 2019QH06).

**Acknowledgments:** The authors appreciate State Key Laboratory of Multiphase Complex Systems and National Natural Science Foundation for their funding and support.

**Conflicts of Interest:** The authors declare no conflict of interest.

#### Nomenclature

BSR	bio-oil derived from straw and husk pyrolysis
BPA	bio-oil from pyrolygneous acid
BFT	bio-oil derived from fruit trees pyrolysis
$T_{m1}$	the temperature at the maximum weight loss rate in stage 1
$T_{m2}$	the temperature at the maximum weight loss rate in stage 2
$T_{m3}$	the temperature at the maximum weight loss rate in stage 3
$T_f$	the final weight loss temperature
E	activation energy
A	frequency factor

#### References

1. Trippe, F.; Fröhling, M.; Schultmann, F.; Stahl, R.; Henrich, E. Techno-economic assessment of gasification as a process step within biomass-to-liquid (BtL) fuel and chemicals production. *Fuel Process. Technol.* **2011**, *92*, 2169–2184. [CrossRef]
2. Chhiti, Y.; Salvador, S.; Commandré, J.-M.; Broust, F.; Couhert, C. Wood Bio-Oil Noncatalytic Gasification: Influence of Temperature, Dilution by an Alcohol and Ash Content. *Energy Fuels* **2011**, *25*, 345–351. [CrossRef]
3. Lu, Q.; Li, W.; Zhu, X. Overview of fuel properties of biomass fast pyrolysis oils. *Energy Convers. Manag.* **2009**, *50*, 1376–1383. [CrossRef]

4. Feng, P.; Hao, L.; Huo, C.; Wang, Z.; Lin, W.; Song, W. Rheological behavior of coal bio-oil slurries. *Energy* **2014**, *66*, 744–749. [[CrossRef](#)]
5. Dahmen, N.; Henrich, E.; Dinjus, E.; Weirich, F. The bioliq<sup>®</sup> bioslurry gasification process for the production of biosynfuels, organic chemicals, and energy. *Energy Sustain. Soc.* **2012**, *2*, 3. [[CrossRef](#)]
6. Zhang, M.; Liaw, S.B.; Wu, H. Bioslurry as a Fuel. 5. Fuel Properties Evolution and Aging during Bioslurry Storage. *Energy Fuels* **2013**, *27*, 7560–7568. [[CrossRef](#)]
7. Guo, F.; Guo, Y.; Guo, Z.; Miao, Z.; Zhao, X.; Zhang, Y.; Li, J.; Wu, J. Recycling Residual Carbon from Gasification Fine Slag and Its Application for Preparing Slurry Fuels. *ACS Sustain. Chem. Eng.* **2020**, *8*, 8830–8839. [[CrossRef](#)]
8. Zhang, Y.; Kajitani, S.; Ashizawa, M.; Oki, Y. Tar destruction and coke formation during rapid pyrolysis and gasification of biomass in a drop-tube furnace. *Fuel* **2010**, *89*, 302–309. [[CrossRef](#)]
9. Feng, P.; Lin, W.; Jensen, P.A.; Song, W.; Hao, L.; Raffelt, K.; Dam-Johansen, K. Entrained flow gasification of coal/bio-oil slurries. *Energy* **2016**, *111*, 793–802. [[CrossRef](#)]
10. Feng, P.; Lin, W.; Jensen, P.A.; Song, W.; Hao, L.; Li, S.; Dam-Johansen, K. Characterization of Solid Residues from Entrained Flow Gasification of Coal Bio-Oil Slurry. *Energy Fuels* **2020**, *34*, 5900–5906. [[CrossRef](#)]
11. Raffelt, K.; Henrich, E.; Koegel, A.; Stahl, R.; Steinhardt, J.; Weirich, F. The BTL2 Process of Biomass Utilization Entrained-Flow Gasification of Pyrolyzed Biomass Slurries. *Appl. Biochem. Biotechnol.* **2006**, *129*, 153–164. [[CrossRef](#)]
12. Wu, H.; Yu, Y.; Yip, K. Bioslurry as a Fuel. 1. Viability of a Bioslurry-Based Bioenergy Supply Chain for Mallee Biomass in Western Australia. *Energy Fuels* **2010**, *24*, 5652–5659. [[CrossRef](#)]
13. Abdullah, H.; Mourant, D.; Li, C.-Z.; Wu, H. Bioslurry as a Fuel. 3. Fuel and Rheological Properties of Bioslurry Prepared from the Bio-oil and Biochar of Mallee Biomass Fast Pyrolysis. *Energy Fuels* **2010**, *24*, 5669–5676. [[CrossRef](#)]
14. Abdullah, H.; Wu, H. Bioslurry as a Fuel. 4. Preparation of Bioslurry Fuels from Biochar and the Bio-oil-Rich Fractions after Bio-oil/Biodiesel Extraction. *Energy Fuels* **2011**, *25*, 1759–1771. [[CrossRef](#)]
15. Gao, W.; Zhang, M.; Wu, H. Fuel properties and ageing of bioslurry prepared from glycerol/methanol/bio-oil blend and biochar. *Fuel* **2016**, *176*, 72–77. [[CrossRef](#)]
16. Sakaguchi, M.; Watkinson, A.P.; Ellis, N. Steam Gasification of Bio-Oil and Bio-Oil/Char Slurry in a Fluidized Bed Reactor. *Energy Fuels* **2010**, *24*, 5181–5189. [[CrossRef](#)]
17. Svoboda, K.; Pohořelý, M.; Jeremiáš, M.; Kameníková, P.; Hartman, M.; Skoblja, S.; Huber, F. Fluidized bed gasification of coal–oil and coal–water–oil slurries by oxygen–steam and oxygen–CO<sub>2</sub> mixtures. *Fuel Process. Technol.* **2012**, *95*, 16–26. [[CrossRef](#)]
18. Ruoppolo, G.; Cante, A.; Chirone, R.; Miccio, F.; Stanzione, V. Fluidized bed gasification of coal/biomass slurries. *Chem. Eng. Trans.* **2011**, *24*, 13–18.
19. Dash, U.; Dash, U.; Nayak, A.; Misra, P.K. Surface Engineering of Low Rank Indian Coals by Starch-Based Additives for the Formulation of Concentrated Coal–Water Slurry. *Energy Fuels* **2010**, *24*, 1260–1268. [[CrossRef](#)]
20. Huang, J.; Xu, J.; Wang, N.; Li, L.; Guo, X. Effects of Amphiphilic Copolymer Dispersants on Rheology and Stability of Coal Water Slurry. *Ind. Eng. Chem. Res.* **2013**, *52*, 8427–8435. [[CrossRef](#)]
21. Dash, U.; Dash, U.; Meher, J.; Misra, P.K. Improving stability of concentrated coal–water slurry using mixture of a natural and synthetic surfactants. *Fuel Process. Technol.* **2013**, *113*, 41–51. [[CrossRef](#)]
22. Liu, Z.; Wang, Q. Calculation and confirmation of the kinetic triplet of metallurgical coke gasification with carbon dioxide under isothermal conditions. *J. Therm. Anal. Calorim.* **2019**, *139*, 2235–2241. [[CrossRef](#)]
23. Di Blasi, C. Combustion and gasification rates of lignocellulosic chars. *Prog. Energy Combust. Sci.* **2009**, *35*, 121–140. [[CrossRef](#)]
24. Slezak, R.; Krzystek, L.; Ledakowicz, S. CO<sub>2</sub> gasification of char from spent mushroom substrate in TG-MS system. *J. Therm. Anal. Calorim.* **2019**, *140*, 2337–2345. [[CrossRef](#)]
25. Creager, N.; Brown, R.C. High pressure, oxygen blown entrained-flow gasification of bio-oil. In Proceedings of the International Conference on Thermochemical Conversion of Biomass, Chicago, IL, USA, 3–6 September 2013.
26. Chhiti, Y.; Salvador, S. Gasification of wood bio-oil. In *Gasification for Practical Applications*; Yun, Y., Ed.; InTech: London, UK, 2012. [[CrossRef](#)]

27. Chhiti, Y. Non Catalytic Steam Gasification of Wood Bio-Oil. Ph.D. Thesis, Univerite du Toulouse, Toulouse, France, 5 September 2011.
28. Noumi, E.S.; Blin, J.; Valette, J.; Rousset, P. Combined Effect of Pyrolysis Pressure and Temperature on the Yield and CO<sub>2</sub> Gasification Reactivity of Acacia Wood in macro-TG. *Energy Fuels* **2015**, *29*, 7301–7308. [[CrossRef](#)]



© 2020 by the authors. Licensee MDPI, Basel, Switzerland. This article is an open access article distributed under the terms and conditions of the Creative Commons Attribution (CC BY) license (<http://creativecommons.org/licenses/by/4.0/>).